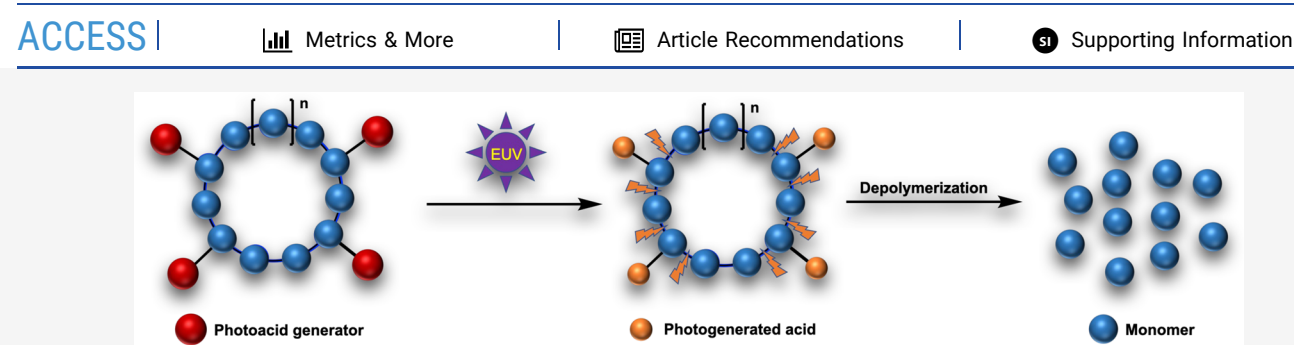


pubs.acs.org/JACS Article

Modular Synthesis of Phthalaldehyde Derivatives Enabling Access to Photoacid Generator-Bound Self-Immolative Polymer Resists with Next-Generation Photolithographic Properties

Jingyuan Deng,* Sean Bailey, Shaoyi Jiang, and Christopher K. Ober*





ABSTRACT: The resolution, line edge roughness, and sensitivity (RLS) trade-off has fundamentally limited the lithographic performance of chemically amplified resists. Production of next-generation transistors using extreme ultraviolet (EUV) lithography depends on a solution to this problem. A resist that simultaneously increases the effective reaction radius of its photogenerated acids while limiting their diffusion radius should provide an elegant solution to the RLS barrier. Here, we describe a generalized synthetic approach to phthalaldehyde derivatives using sulfur(VI) fluoride exchange click chemistry that dramatically expands usable chemical space by enabling virtually any non-ionic photoacid generator (PAG) to be tethered to phthalaldehyde. The resulting polymers represent the first ever PAG-tethered self-immolative resists in an architecture that simultaneously displays high contrast, extraordinary sensitivity, and low roughness under EUV exposure. We believe this class of resists will ultimately enable researchers to overcome the RLS trade-off.

■ INTRODUCTION

Development of new polymer-based resists has undergone a renaissance in the last 5 years due to the adoption of extreme ultraviolet (EUV) lithography as the premiere lithographic technology necessary for further reductions in transistor feature size.^{1,2} The decade prior to 2015 was characterized by few new advances in resist chemistry³ as the lifespan of 193 nm lithography was extended using breakthroughs in immersion optics⁴ and phase-shifting masks⁵ that required minimal changes to previously established materials.⁶⁻⁸ In contrast, the 13.5 nm wavelength used in EUV sources has transformed the exposure mechanism from well-understood selective photon absorption to indiscriminate ionization of a resist to generate secondary electrons. These secondary electrons move through the resist and are responsible for the ensuing chemical reactions. Additionally, the low power output of EUV sources has mandated the use of high-sensitivity resists to achieve sufficient throughput and lower costs. Such stringent sensitivity requirements must be met while maintaining the ability to print ever-shrinking critical dimensions. This confluence of challenges has triggered a flurry of research into new EUV chemistries, ¹⁰⁻¹² resist additives, ¹³⁻¹⁵ and material architectures. ¹⁶⁻²² However, chemically amplified resists (CARs)²³ continue to dominate the commercial EUV resist market.

CARs utilize photoacid generators (PAGs) to produce acid that can catalytically remove protecting groups on the polymer chain, ^{24,25} triggering a solubility gradient between the exposed and unexposed areas of the resist. As the generation of a single molecule of acid can lead to numerous deprotection events, the sensitivity of the resist is significantly amplified. Further improvements to modern CARs are extraordinarily challenging to introduce due to the difficulty in simultaneously optimizing the resolution, line edge roughness, and sensitivity (RLS tradeoff). ^{26,27} It would require both the effective reaction radius of the resist and the activation energy for diffusion of the acid to be increased. These two conditions appear to be at odds with one another, and unsurprisingly, the RLS trade-off has grown into the foremost problem hampering the development of new

Received: August 2, 2022



Previous work Depolymerization Depolymerization This work Monomer repeating unit Depolymerization Photoacid generate Photoactive end-cap

Figure 1. (a) Linear PPA with PAG blending. (b) PPA with photoactive end-cap. (c) Functionalized cyclic PPA with PAG tethering.

EUV resists. Stochastic issues related to the mixing of the polymer and PAGs accentuate the RLS trade-off by promoting inhomogeneous acid distribution that requires increased diffusion to smooth out.²⁸

Retarding acid diffusion as a means of overcoming the RLS trade-off has seen some success through incorporation of the PAG into the polymer. Initially, resists that integrated PAGs into the main chain were designed to only enable high PAG loadings in the absence of phase separation.^{29,30} These PAGs were straightforward to synthesize but still dissociated into acids that could diffuse without restriction. Once it was demonstrated that PAGs possessing anions which remained bound to the polymer could reduce the acid diffusion length sevenfold,³¹ numerous bound anionic PAGs were designed, ^{32–35} and a significant reduction in line edge roughness was noted in nearly every case. Critically, the photospeed of these polymer-bound PAGs was either comparable or inferior to the photospeed of an unbound PAG blend of the same concentration. This meant that ionic PAGs and thick films had to be employed to absorb sufficient EUV radiation. Films thicker than 50 nanometers suffer dramatic reductions in resolution due to pattern collapse,³⁶ and ionic PAGs such as triphenylsulfonium triflate are dogged by a poor out-of-band response that adversely impacts contrast.³

A second major initiative to overcome the RLS trade-off was through the advancement of self-immolative polymers.³⁸⁻⁴⁰ These resists possess an alternative source of chemical amplification, and it was anticipated that the lack of acid diffusion would lead to simultaneous improvement of the RLS parameters. Examples include poly(olefin sulfones), 41,42 poly-(esters), 43,44 and poly(acetals). 45-47 While many self-immolative resists are unable to achieve sensitivities comparable to typical CARs, a class of poly(acetals), poly(phthalaldehyde) (PPA), has proven to be one of the most promising due to its unprecedented rate of depolymerization in the solid phase. Unfortunately, PPA and related materials are afflicted with a tendency to contaminate the optics of EUV instruments and a lack of bench stability.

Recently, we reported the synthesis of a thermally stable brominated PPA resist with extremely low levels of outgassing. 48-50 This polymer was blended with novel PAGs and achieved sensitivities as low as 12 mJ/cm² under EUV radiation. Our attempt to further improve this resist system by eliminating PAGs and relying only on the scission of a radiation responsive end-cap to initiate depolymerization was moderately successful as the photospeed of the material reached 90 mJ/cm^{2.51} Rather than further pursue a PAG-free strategy, we reasoned that functionalizing a PPA monomer with different non-ionic PAGs would enable us to take advantage of the roughness reduction witnessed in many polymer-bound PAG resists (Figure 1). This reduction could also enable high sensitivity and contrast due to a dual amplification mechanism through use of non-ionic PAGs. No single component resist commanding two different forms of chemical amplification has been previously reported, considering the well-known difficulty in synthesizing functionalized phthalaldehydes .52,53

Herein, we report the development of a versatile synthetic strategy using sulfur(VI) fluoride exchange (SuFEx) click chemistry⁵⁴ to prepare EUV-active PPA derivatives with highly sensitive functional groups that are otherwise inaccessible through conventional methods. Polymerization of these derivatives yielded the first PAG-tethered self-immolative resists that displayed unprecedented photospeed, contrast and low roughness under EUV exposure.

■ RESULTS AND DISCUSSION

PAG Design. Numerous classes of non-ionic PAGs exist, including aryl sulfonates, diazo sulfones, and nitrobenzyl sulfonates. However, only imido sulfonates and imino sulfonates have proven to be sufficiently sensitive to EUV radiation.⁵⁵ Based on our initial work demonstrating that imido sulfonates and imino sulfonates with extended conjugation systems possessed favorable reduction potentials critical for the attachment of secondary electrons, 48 we designed highly EUV-

Scheme 1. Chemical Structures of PAG 1 to 4

Scheme 2. Proposed Degradation Pathway for PAG 1

active PAGs using N-aryl imino sulfonate and naphthalimide structures (Scheme 1). Our initial synthesis of the N-aryl imino sulfonate PAGs was complicated by stability issues. Upon isolation, PAG 1 was a white crystalline solid but became yellow and sticky within 12 h on the benchtop. The degradation process was monitored by ¹H NMR spectral change in CDCl₃. In the nuclear magnetic resonance (NMR) spectra (Supporting Information, Figure S11), we observed formation of sulfonic acid as indicated by the peak at 12.4 ppm. The water peak was also shifted downfield and broadened, signifying interaction between the residual water and sulfonic acid. The presence of sulfonic acid was confirmed by DART-MS of PAG 1 after 48 h of isolation (Supporting Information, Figure S15). There are two possible pathways of generating sulfonic acid from PAG 1. One requires N-O bond cleavage. This seemed extremely improbable as the N-O bond will not cleave without any applied stimuli (such as radiation), and high stability of PAG 2 would be impossible. The other possible pathway is through a Beckman-type rearrangement as proposed in Scheme 2. A similar rearrangement was previously reported for the reaction of α -hydroxyimino-ketones with ptoluenesulfonyl chloride. 56 ¹H NMR analysis of PAG 1 after 23 days of isolation unambiguously showed that 4-bromoacetanilide is the sole rearrangement product (Supporting Information, Figures S12 and S13), indicating that only the aryl group migrated. The proposed degradation pathway was further supported by DART-MS of PAG 1 after 48 h of isolation (Supporting Information, Figure S14). Mass peaks were found that corresponded to the molecular ion of 4-bromoacetanilide and the nitrilium ion intermediate. We anticipated that a

sufficiently electron-withdrawing substituent could destabilize the nitrilium intermediate. A trifluoromethyl group was selected for this purpose with the added benefit of increasing the EUV absorption cross section ^{57,58} of the PAG. Fortuitously, we found PAG 2 to be completely bench-stable for more than 2 years. Its increased stability can also be seen in DART–MS as the molecular ion of PAG 2 was observable, which was not possible for PAG 1 even immediately after isolation (Supporting Information, Figure S16). PAG 3 was synthesized without bromination on the para position of the *N*-aryl ring to probe the effect of the PAG reduction potential on single component resists. The naphthalimide-based PAG 4 did not suffer from any stability issues.

We had previously observed a highly unusual degradation pathway for PAG 4 that involved the simultaneous generation of acid and base.⁴⁸ We were concerned that PAG 2 could undergo a similar mechanism, which would negatively impact the sensitivity of the resist. Therefore, EUV exposure experiments were conducted by mixing PAG 2 with brominated linear PPA (Br-lPPA) to elucidate its behavior under EUV radiation. A wafer coated with the Br-IPPA resist and PAG 2 was exposed to EUV radiation at a dosage of 12 mJ/cm² and post-baked at 110 °C for 1 min. The wafer was then developed in isopropanol for 1 min. The development solution was concentrated in vacuo and used for direct analysis in real time (DART)-MS analysis. From the mass spectra (Supporting Information, Figures S17-S19), we observed peaks corresponding to the brominated monomer under positive-ion mode and peaks corresponding to sulfonic acid and the isopropanol adduct of 4-bromo-trifluoromethylaceto-

Scheme 3. Proposed Decomposition Mechanism of PAG 2 under EUV Radiation

Scheme 4. Synthesis of Aryl Sulfonate PAG-Tethered Phthalaldehyde

phenone under negative-ion mode. Based on these findings, the proposed degradation pathway is shown in Scheme 3. PAG 2 forms an imine species after hydrogen abstraction that is highly prone to hydrolysis in the presence of water vapor from the environment. The final result is a chemically unreactive ketone and ammonia gas that is quickly lost to the surrounding atmosphere. This is in sharp contrast to PAG 4, which generates a stable solid base. With these stable and EUV-active PAGs in hand, we moved on to the construction of a single component resist by tethering these PAGs to the brominated monomer.

Synthesis of PAG-Tethered Monomers and Polymers. Significant effort and research have been devoted to finding applications for o-phthalaldehyde (o-PA) in the past decades as it is easily accessible via commercial suppliers. 59-63 Functionalized o-PA is very rarely reported as the synthesis is challenging and tedious,53 often requiring multiple lowyielding steps. Two methods to access substituted PPAs have been reported in the literature. First, functionalized o-PAs have been prepared by synthesizing the related diols and oxidizing them to form the dialdehyde. 52 The synthetic routes suffered from low yielding steps and necessitated the usage of redox reactions that would not tolerate the labile functional groups key to EUV activity. Second, copolymerization of functionalized benzaldehydes with o-PA has proven to be a successful method to obtain substituted PPA.⁶⁴ The limitation of this methodology lies in the low incorporation ratio of the

functionalized benzaldehydes and poor polymerization yield. A theoretically possible strategy to synthesize derivatized PPA is to perform post-polymerization functionalization on PPA using reactive side-chain groups on the polymer backbone. However, this did not seem feasible as PPA would be prone to decomposition during the process due to its metastability, especially considering that many post-polymerization reactions require either prolonged reaction times or elevated temperatures to achieve reasonable yields. In this work, we sought to unlock the first synthetic access to PAG-tethered self-immolative polymers by developing a new, modular approach to the synthesis of *o*-PA derivatives using mild conditions that would be compatible with sensitive EUV motifs.

We first envisioned accomplishing these goals by employing cross-coupling chemistry on brominated o-PA to establish a generalized route for the incorporation of EUV-active groups. The monomer synthesis began by treating commercially available 4-bromophthalic acid with borane to afford the diol followed by Swern oxidation to the brominated dialdehyde in 76% yield (two steps). Crucially, we found that mineral impurities that significantly disrupted subsequent steps had to be removed using vacuum sublimation as chromatography proved insufficient. A condensation reaction between 4-hydroxyacetophenone and 4-bromobenzenesulfonyl chloride yielded the brominated PAG precursor that then underwent Miyaura borylation to give the initial boronic ester coupling partner of the dialdehyde. Attempted Suzuki–Miyaura

coupling on 4-bromo phthalaldehyde (Scheme 4) failed to produce the desired product and instead resulted in a complex mixture of high molecular weight di-brominated species. It was apparent that a form of cross linking was occurring between the dialdehyde functional groups.

Eliminating this problem necessitated the protection of the dialdehyde moiety. Protection to an imine would be ideal as the resulting product would likely be crystalline and therefore facile to purify. Additionally, an imine-protected aldehyde could potentially undergo an iridium-catalyzed meta C–H borylation reaction⁶⁵ such that functionalized phthalaldehyde could be synthesized directly from the commercially available original phthalaldehyde. Attempted protection failed as the initial formation of the imine on one aldehyde group resulted in cyclization to a stable five-membered ring, leaving the remaining aldehyde group in its hemiacetal form.

Following this initial setback, we employed the diacetal protecting group shown in Scheme 5. From the crude NMR

Scheme 5. Synthesis of Diacetal-Protected Brominated Phthalaldehyde

spectrum, two diastereomers, cis and trans, were observed. Surprisingly, we were able to recrystallize one of the isomers from this mixture despite the infamous reputation acetalprotecting groups have for promoting the formation of amorphous substances. This compelled us to determine the relative stereochemistry of the isolated diastereomer. We were able to determine the identity of the diastereomer by combining two-dimensional (2D) nuclear Overhauser effect spectroscopy (NOESY) and 2D 13C-coupled 1H/13C heteronuclear single quantum coherence spectroscopy (HSQC)-NOESY NMR experiments on the mixture of both isomers. The detailed analysis is given in the Supporting Information, pages S27-S32. The trans isomer was determined to be crystalline and was exclusively used for all the derivatization reactions for NMR simplicity and convenience in weighing throughout this work. It should be noted that the cis isomer can also be furnished in high purity via distillation.

Using the previously synthesized boronic ester PAG, we successfully obtained the biaryl product using Suzuki–Miyaura coupling with the phthalaldehyde diacetal. The chemical activity of each isomer was evaluated, and no reactivity difference was found.

We screened different ligands and Pd precursors to optimize the reaction yield as shown in the Supporting Information,

Table S1. Among all of the conditions tested, tris(1adamantyl)phosphine (P(Ad)₃) in combination with Pd₂dba₃ was the only one capable of providing a sufficient yield of 67% in comparison to the less than 25% yield afforded by alternative ligands (Scheme 6). P(Ad)3 had previously been devised to possess an excellent electron-releasing character and a robust catalytic performance in various Pd-catalyzed reactions. 66,67 Presumably, the diacetal-protected phthalaladehyde was electron-rich enough to inhibit oxidative addition by Pd, and this was able to be overcome with a sufficiently powerful ligand. Our previous work showed that the S-O bond in aryl sulfonate PAGs was not sufficiently weak to be cleaved under EUV radiation despite possessing excellent DUV activity.48 Thus, we moved onto the more difficult and sensitive imido and imino sulfonates. Unfortunately, the boronic ester of PAG 4 could not be formed via Miyaura borylation. Suzuki-Miyaura coupling between the borylated phthalaldehyde diacetal and brominated PAG 4 (Scheme 7) also failed to give any product. We hypothesized that Pd could be inserting into the N-O bond, which is supported by a previous work in which the authors isolated the oxidative addition product during the development of a Pd-catalyzed amination reaction using oxime esters. ⁶⁸ Pd-catalyzed reactions were thus abandoned in favor of metal-free alternatives.

Our next trial focused on the catalytic SuFEx reaction, a highly selective and rapid click chemistry developed in 2014.⁵⁴ We first built the sulfonyl fluoride moiety onto the protected phthalaldehyde diacetal using conditions designed during our previously successful Suzuki-Miyaura coupling reaction conducted on the diacetal-protected brominated phthalaldehyde. Scheme 8 shows that we successfully cross-coupled 4-(fluorosulfonyl)phenylboronic acid to obtain 4-benzenesulfonyl fluoride phthalaldehyde diacetal (SuFDA). Traditionally, SuFEx reactions have utilized H⁺, R₃Si⁺, and/or organic bases such as tertiary amines, amidines, and phosphazenes to activate the sulfonyl fluoride, transforming it from a strong covalent bond to a leaving group. More recently, an accelerated SuFEx click chemistry was conceived for coupling aryl and alkyl alcohols with SuFExable hubs utilizing Barton's hindered guanidine base, 2-tert-butyl-1,1,3,3-tetramethylguanidine and hexamethyldisilazane as a silylating reagent to activate sulfonyl fluoride.69

We adapted this reaction condition to synthesize an imido PAG-tethered phthalaldehyde diacetal as shown in Scheme 9. The reaction generated the desired product in 81% yield even though the coupling partner was not an aryl or alkyl alcohol. We also employed the same reaction conditions to construct the previously synthesized aryl sulfonate PAG-tethered phthalaldehyde diacetal using a commercially available phenol as shown in Scheme 10. The reaction was conducted at ambient temperature and finished within 30 min with over 90% isolated yield. On comparing SuFEx click chemistry with our optimized Suzuki—Miyaura coupling, it is obvious that

Scheme 6. Synthesis of Aryl Sulfonate PAG-Tethered Phthalaldehyde Diacetal

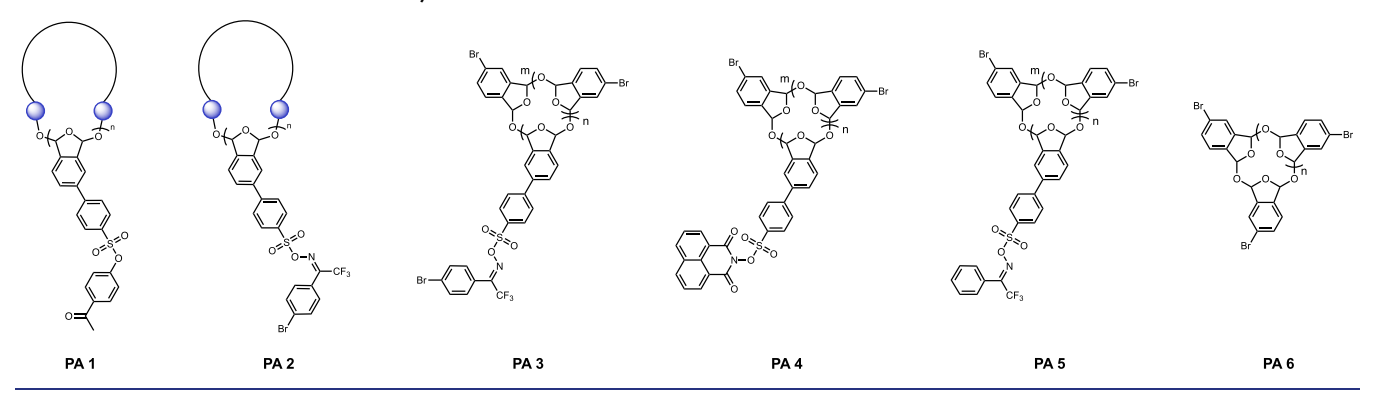
Scheme 7. Attempted Suzuki-Miyaura Coupling on PAG 4

Scheme 8. Synthesis of 4-Benzenesulfonyl Fluoride Phthalaldehyde Diacetal

Scheme 9. Synthesis of Imido PAG-Tethered Phthalaldehyde Diacetal

Scheme 10. Synthesis of PAG-Tethered Phthalaldehydes through SuFEx

Scheme 11. Chemical Structures of Synthesized PAG-Tethered PPAs



SuFEx click chemistry is superior for tethering PAGs as it does not use metals, requires a lower reaction temperature and shorter reaction time, and provides a higher yield. Because almost all known non-ionic PAGs (both DUV and EUV) are derivatizations of sulfones,⁵⁵ this methodology provides a general route to an entire class of previously synthetically inaccessible materials. Additionally, the broadly available commercial SuFExable substrates, including amines and

alcohols, strongly suggest that the synthetic strategy we developed could be used to create a wide variety of phthalaldehyde derivatives that may possess unique properties ($T_{\rm c}$ /stability, mechanical properties, and so forth) for different applications.

We applied the same SuFEx reaction conditions to couple imino and imido oximes with sulfonyl fluoride as shown in Scheme 10. The reaction worked efficiently in all cases and generated the corresponding imino and imido PAG-tethered phthalaldehyde diacetals in yields of 81–86%. The dialdehyde groups were reintroduced using mild acid-catalyzed hydrolysis on the PAG-tethered phthalaldehyde diacetals to give PAG-tethered phthalaldehydes DA 1, 2, 3, and 4 in high yield.

With DA 1, 2, 3, and 4 in hand, we synthesized cyclic homopolymers of PA 1 and PA 2 as shown in Scheme 11 through cationic polymerization reactions. We discovered that PA 2 was too sensitive (<1 mJ/cm² photospeed) under EUV radiation to properly evaluate its lithographic properties with the tools accessible to us. Therefore, we synthesized copolymers PA 3, 4, and 5 as shown in Scheme 11 by mixing 10 mol % of PAG-tethered phthalaldehydes with brominated phthalaldehydes. The incorporation ratio of the PAG-tethered monomers in the copolymer was calculated by dissolving the copolymer in CDCl₃ and allowing the residual DCl to trigger depolymerization. The integration ratio between the two different dialdehyde proton peaks was interpreted as the ratio of the incorporated PAG-tethered monomers in the copolymer. We chose this ratio to compare the sensitivity between the single-component system in this work and the twocomponent system in our previous work where the mixed PAG ratio to the monomer was also 10 mol %. The nearly identical feed ratio and copolymer composition suggests either an alternating or a statistical sequence as previously observed by other groups.⁵² Surprisingly, PA 2, 3, 4, and 5 possessed excellent thermal stability, with $T_{\rm d}$ ranging from 153 to 203 °C (Supporting Information, Figures S1–S3). Additionally, these polymers were found to be stable at room temperature over 1 month as we did not observe any degradation via NMR. This sharply contrasted with the brominated cyclic polyphthalaldehyde homopolymer, which started to decompose in less than 1 month. There are two possible reasons that could lead to this improved stability. The first is likely due to the strong electronwithdrawing character of the PAG moiety. According to prior research, phthalaldehyde derivatives with strong electronwithdrawing groups displayed higher experimentally determined ceiling temperatures. ⁵² Ceiling temperatures could also be calculated through density functional theory (DFT) based on the assumption that ΔS remains constant for different monomers. Although the calculated values are not quantitatively accurate, they can help us qualitatively estimate ceiling temperature based on thermodynamic parameters and see a rough trend. We calculated the ceiling temperatures based on the assumption that ΔS remains constant for different monomers, and the results are summarized in Table S2 of the Supporting Information. Cyclic brominated PPA had a calculated T_c of -22 °C, whereas homo PPA polymerized from DA 4, DA 3, and DA 2 had calculated T_c values of -5, 13, and 2 °C, respectively. The calculated ceiling temperatures were thus found to be strongly correlated to the electronwithdrawing character of different PAG moieties and the overall stability of each polymer. The second is presumably due to the residual Lewis acid from the polymerization reactions. The imino and imido groups on the PAG-tethered derivatives

could behave as Lewis bases, which sequester residual Lewis acid left over from the polymerization reactions and thus enhance the stability of the material. PA 6 ($T_{\rm d}$: 158 °C), the cyclic homopolymer of brominated phthalaldehyde, only has acetal oxygens that can behave as Lewis bases to sequester residual Lewis acid, and consequentially the polymer has a shorter shelf life. This reasoning is also supported by our previous work⁴⁸ as the linear homopolymer of brominated phthalaldehyde, which was prepared without Lewis acid, has a higher $T_{\rm d}$ (178 °C).

The literature offers several outstanding examples of polymers with high EUV activity. We provide a comparison here that illustrates the novelty of our methodology and its advantages to previously published work on chain scissionable materials. The prior synthetic approaches may be divided into multiple classes including poly(olefin sulfone)s, 41,42 poly-(esters), 44,70 poly(carbonates), 71,72 and poly(acetals). 46 Poly-(esters), poly(carbonates), and poly(acetals) are synthesized via step-growth polymerization, which severely limits their conversion and dispersity. In contrast, we were able to employ ionic polymerization with our monomers to circumvent these obstacles. Notably, the reactivity of the diastereomers of our monomers was of no impact to the synthesis, whereas prior work on poly(esters)⁴⁴ suffered from having to isolate one diastereomer to ensure a high yield during the polymerization process. Our route also managed to completely exclude the usage of copper during polymerization, which is significant as single-digit parts per million levels of copper can result in disastrous device defects.⁷³ In contrast, work on poly(olefin sulfone)s⁴² required the usage of copper in their atom transfer radical polymerization, which would make it extremely challenging, if not impossible, to reach acceptable copper contaminant levels in these resists. Additionally, the storage stability of our precursors is not dependent on air- or moisturefree conditions, which plagued the bis-carbonylimidazolide monomers required in the synthesis of EUV-active poly-(carbonates). Lastly, all preceding literature on PAGtethered polymers (both anionic and cationic) has required completely new synthetic routes for each derivative, 33,74-76 whereas our route can incorporate an entire library of covalent PAGs from a single parent building block.

EUV Exposure. A resist's resolving power is dependent on its ability to quickly transition between insolubility and complete solubility over a narrow range of exposure doses. As EUV resists are characteristically thin due to processing requirements, the thickness of the resist after development T(x) may be assumed to be determined by the dose alone.⁷⁷ Exposing areas of a resist coated on a wafer to different doses and evaluating the remaining thickness after development is the basis of the contrast curve. The curve is plotted using the residual thickness at a specific dose T(E) normalized to the initial thickness T(0). Formally, the contrast γ is defined as $T(E)/T(0) = \gamma \log(E_0/E)$ where E_0 is the dose to clear and $E < \infty$ E_0 is taken from the linear region within the vicinity E_0 . The standard procedure given by ASTM F1059-87 allows for a more well-defined measure of γ using a least squares regression analysis between the points at which T(x)/T(0) is equal to 0.7 and 0.1. γ is also critical to another important aspect of the resist profile: the sidewall angle, which affects the ability of the etching process to differentiate between the exposed and unexposed regions of the resist. ⁷⁸ An ideal photoresist profile will possess a sidewall angle θ of 90° to minimize the rate at which the critical dimension is altered during the etching

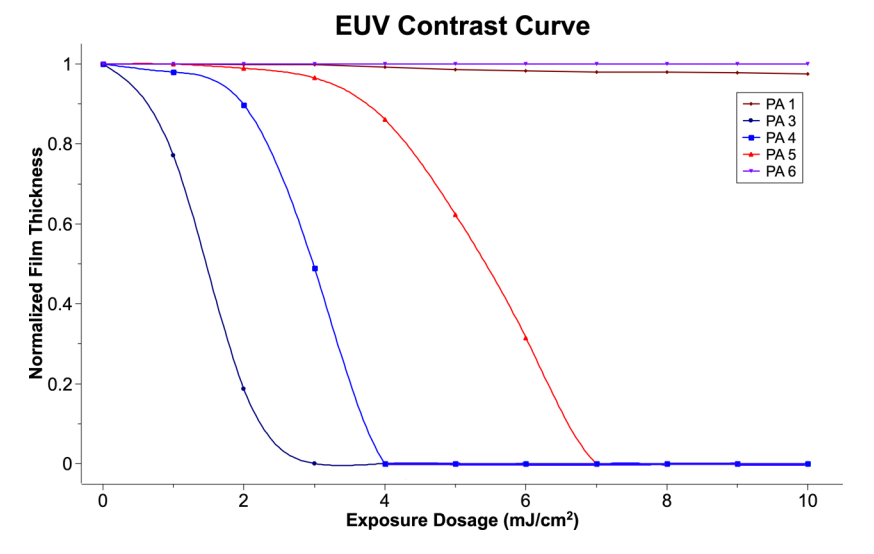


Figure 2. EUV contrast curve for PA 1 to PA 6.

process, and the sidewall angle is related to the contrast through $tan(\theta) = [-T(0)\gamma/E(x)][dE(x)/dx]$ where E(x) is the exposure dose at distance x across the resist image.⁷⁷ Thus, γ may be viewed as a crucial metric for evaluating the performance of high-resolution resists. Contrast curve measurements were made by first dissolving each resist polymer (35 mg) in 1 mL of γ -butyrolactone. The solutions were spin-coated onto a silicon wafer at 2000 rpm for 1 min, resulting in film thicknesses of 40 nm, and then soft baked on a hot plate at 70 °C for 1 min to remove the residual casting solvent from the film. After EUV exposure, each wafer was postexposure-baked at 110 °C for 1 min and developed in isopropanol for 1 min. Using the ASTM F1059-87 definition of contrast, we found γ to be 2.74 for PA 4 and 3.74 for PA 5 (Supporting Information, Figure S37). These are excellent contrast values as commercial resists typically command γ values in the range of 2-3.79 Since the contrast curve tool could only measure doses in integer values, we could not accurately determine γ for PA 3 due to its exceptionally low E_0 . As previously mentioned, minimizing E_0 is vital for resists to achieve high throughput on low-power EUV sources. The EUV contrast curves (Figure 2) show that the sensitivities of PA 3, 4, and 5 were 3, 4, and 7 mJ/cm², respectively. PA 6 was used as a control. To the best of our knowledge, a dose to clear of 3 mJ/cm² is the lowest value reported in the literature for singlecomponent EUV resists to date. This is especially significant as comparable works have relied on multi-component resists, 80-82 which suffer from stochastic problems, and ionic PAGs that have poor out-of-band responses to achieve similar sensitivity. 80,82 As with the two-component version of PA 1, no chemical amplification was observed with the aryl sulfonate moiety, providing more evidence that a highly UV active group can be completely inactive under EUV exposure. It is important to note that the previously encountered base quencher effect⁴⁸ for PAG 4 was not observed in the corresponding PAG-tethered resist PA 4. The quencher had been shown to improve roughness at the expense of contrast. As tethering the PAGs rendered this roughness improvement unnecessary, it was especially convenient that the effect was no longer present. This was likely due to the fact that the generated acids were prevented from diffusing away from the polymer backbone and encountering the quencher.

Line edge roughness is defined as the standard deviation of the edge of a resist feature relative to an averaged, straight edge. It emerges from a combination of photon and material stochastics, including deprotection efficiency and dark loss. 26 A strong correlation between surface roughness and line edge roughness has been repeatedly demonstrated across multiple forms of exposure and processing conditions. 83-86 Measuring surface roughness after coating and comparing it to the roughness after exposure and development allows the inhomogeneity induced by the resist's initial non-uniformity and adhesion to the substrate to be decoupled from stochastics caused by the efficiency of the resist's chemical amplification reaction as well as reaction disparities driven by dark loss. 86 We conducted surface roughness measurements on PA 3 before coating and after development and compared these with unfunctionalized PPA mixed with an equivalent 10 mol % of PAG 3. The root mean square (RMS) values in Table 1

Table 1. Results of Surface Roughness Measurements

resist system	surface roughness after coating (nm)	surface roughness after development (nm)
PPA + PAG 2	0.26	0.29
PA 3	0.25	0.25

indicate that both the PAG-tethered and PAG-blended systems exhibited outstanding film formation behavior. Most significantly, no increase in roughness was found in PA 3 after exposure and development. This means that the chemically amplified reaction in PA 3 did not result in significant chemical heterogeneity. This observation stands out in the photoresist field as state-of-the-art EUV photoresists typically suffer from at least 1.0 nm of degradation to the RMS roughness in the exposure process alone. It demonstrates that the double amplification mechanism in PA 3 from self-immolation of the polymer and the catalytic reactions between the polymer and photogenerated acids has resulted in extremely efficient formation of the latent image.

DFT Calculations. DFT calculations were conducted to understand the unparalleled EUV sensitivity observed on samples PA 3–5. We used model molecules SC 1–3 to simulate the PAG-tethered polyphthalaldehydes as shown in Figure 3. The primary sensitization mechanism of PAGs under

Figure 3. Model molecules SC 1 to 3 for DFT calculations.

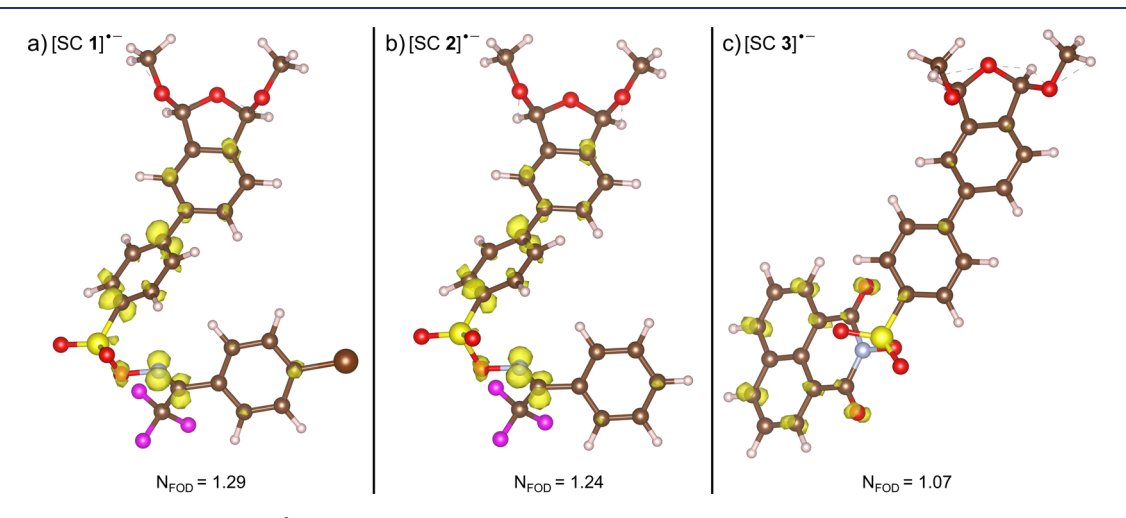


Figure 4. FOD plots at $\sigma = 0.005e$ Bohr⁻³ [FT-B97M-V/def2-TZVPP ($T_{\rm el} = 5000$ K) level] for radical anions of SC 1–3 (FOD in yellow).

EUV radiation begins with the ejection of secondary electrons from the polymer upon absorption of high-energy EUV photons. These mobile electrons diffuse through the resist and are captured by PAGs, generating a radical anion species that decomposes to form an acid and other byproducts. It has been well established that the acid generation yield of a PAG is directly linked to its reduction potential.^{87–89} Furthermore, reduction potentials are linearly related to the vertical electron affinities (VEAs) of the PAGs. 90 Therefore, we sought to calculate the VEAs of SC 1-3 to understand the electron attachment process. We also elected to ascertain bond dissociation energies (BDEs) as they would allow us to discern the ease of PAG decomposition. Conducting standard DFT calculations on radical anion species is very challenging as they display strong static electron correlation (SEC), which cannot be adequately described by standard single-reference DFT as SEC may bring capricious effects into electronic wave functions and derived properties. First, to gauge the strongly correlated and chemically active electrons in the radical anions of the model molecules, fractional occupation numberweighted density (FOD) analysis was performed.⁹¹ The results are shown in Figure 4.

The single size-extensive number, $N_{\rm FOD}$, is the integration of the FOD over all space, which was established to globally quantify SEC. ⁹¹ $N_{\rm FOD}$ for all radical anions is far above an indicative threshold value (0.2) between a single and multireference system, indicating the strong multireference nature of these species. From the FOD plots, significant and delocalized FODs were seen in all radical anions, demonstrating that these species represent true multireference systems. To obtain reliable molecular energies and structures for these multiconfigurational systems, finite-temperature DFT with the

meta-generalized gradient approximation functional TPSS ($T_{\rm el} = 5000~{\rm K}$), 92 combined with D4 dispersion correction, 93 the def2-SVP basis set, and the gCP empirical counterpoise correction were utilized for geometry optimizations and thermal corrections. The final energies were calculated at the FT-B97M-V/def2-TZVPP ($T_{\rm el} = 5000~{\rm K}$) level. 94 The calculated VEAs and BDEs of SC 1–3 are summarized in Table 2. These results are compared with the computed values for the corresponding PAGs 1–4.

Table 2. Table Summarizing Results of VEA, BDE, and Photospeed for SC 1-3 and PAGs 1-4

name	VEA (kcal/mol)	N-O BDE (kcal/mol)	S-O BDE (kcal/mol)	$\begin{array}{c} \text{photospeed}^a \\ \left(\text{mJ/cm}^2\right) \end{array}$
SC 1	48.0	6.26	16.3	3
SC 2	44.1	7.04	17.3	7
SC 3	51.2	9.55	27.7	4
PAG 1	36.6	N/A	N/A	N/A
PAG 2	43.1	14.4	21.6	12
PAG 3	38.6	14.9	22.3	23
PAG 4	49.9	14.1	29.4	15

^aFor SC 1−3, it is the copolymer with PAG-tethered monomer incorporated (i.e., PA 3−5).

A comparison of the calculated VEAs between PAGs 1 and 2 demonstrates the essential use of the CF₃ group as it not only stabilizes the whole chemical structure and enhances the EUV absorption cross section but also sharply increases the VEA. Comparing calculated VEAs and N-O BDEs between SC 1-3 and the corresponding PAGs 2-4, it is evident that in all cases, PAG tethering reduces BDE values and increases VEAs,

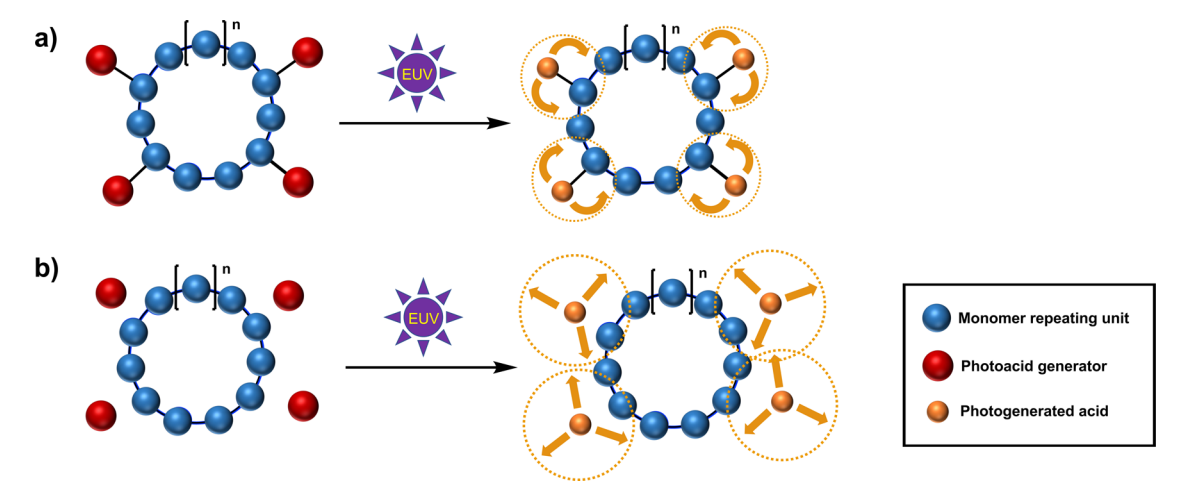


Figure 5. (a) PAGs are tethered with the resist, the photogenerated acid after exposure is confined in vicinity of the reactive polymer backbone with a smaller diffusion radius. (b) PAGs are blended with the resist, the photogenerated acid after exposure diffuses with a larger diffusion radius.

revealing a previously unknown method of sensitivity enhancement. However, the improvements in these thermochemical parameters are unable to fully explain the 3-4-fold improvements in sensitivity. PAG-tethered resists using protecting groups in their solubility switch process do not display such a radical enhancement in photospeed when compared to the corresponding blended resist. Indeed, sensitivity improvements rarely exceed 10%. We propose that our usage of a self-immolative polymer resulted in every photogenerated acid being confined to the vicinity of labile acetal linkages on the polymer backbone as shown in Figure 5. This directly contrasts with a protecting group-based resist in which the randomized distribution of bound PAGs and protecting groups leads to photogenerated acids that may be restricted to a region overlapping with few potential reactive sites.

CONCLUSIONS

PAG-tethered polymers have generated significant interest in the photoresist community as the requirements for state-ofthe-art EUV resists have become increasingly demanding. These resists have thus far been limited to deprotection-based polymers that employ ionic PAGs, which have substantial limitations in terms of stability. In this study, we have demonstrated a modular synthetic approach using SuFEx click chemistry to derivatize o-PA and subsequently provide access to the first PAG-tethered self-immolative polymers. These polymers were found to possess extraordinary sensitivity to EUV radiation, excellent contrast, and unprecedented roughness despite the use of unoptimized processing conditions and non-ionic PAGs. These polymers have been observed to be bench-stable for over a month thus far in contrast to unfunctionalized PPA, which decomposed in the same time frame. DFT calculations helped uncover a previously unknown benefit of tethering PAGs: noteworthy improvements in the thermodynamic parameters relevant to PAG acid generation efficiency. We proposed that the restricted diffusion of every photogenerated acid to the reactive backbone of the polymer was the primary reason for the 3-4-fold enhancement in sensitivity, a synergistic effect never witnessed with prior PAGtethered polymers. We anticipate that the methodology developed in this work will give researchers the opportunity to tether the vast majority of the known PAGs to the o-PA monomers and discover even higher performing resists. Finally, the aforementioned advantageous lithographic properties of these polymers strongly indicate that they would be excellent candidates for the next generation of EUV resists. Patterning experiments utilizing these polymers are ongoing and will be reported in due course.

ASSOCIATED CONTENT

Supporting Information

The Supporting Information is available free of charge at https://pubs.acs.org/doi/10.1021/jacs.2c08202.

General procedures, synthetic and characterization details, thermogravimetric analysis, GPC chromatograms, MS experiments, relative stereochemistry determination, atomic force microscopy measurements, Gamma calculation, NMR spectra, and computational details (PDF)

AUTHOR INFORMATION

Corresponding Authors

Jingyuan Deng — Department of Chemistry and Chemical Biology and Department of Materials Science and Engineering, Cornell University, Ithaca, New York 14853, United States; orcid.org/0000-0002-0858-9919; Email: jd966@cornell.edu

Christopher K. Ober — Department of Materials Science and Engineering, Cornell University, Ithaca, New York 14853, United States; orcid.org/0000-0002-3805-3314; Email: cko3@cornell.edu

Authors

Sean Bailey — Department of Materials Science and Engineering and Department of Biomedical Engineering, Cornell University, Ithaca, New York 14853, United States; orcid.org/0000-0002-0792-210X

Shaoyi Jiang — Department of Materials Science and Engineering and Department of Biomedical Engineering, Cornell University, Ithaca, New York 14853, United States; orcid.org/0000-0001-9863-6899

Complete contact information is available at: https://pubs.acs.org/10.1021/jacs.2c08202

Note:

The authors declare no competing financial interest.

ACKNOWLEDGMENTS

This research was supported by Intel Corporation through the SRC research project (task ID: 2885.001). Exposures were performed by James Blackwell at Intel Corporation and with Greg Denbeaux at SUNY Polytechnic Institute. This work made use of the Cornell Center for Materials Research Shared Facilities, which are supported through the NSF MRSEC program (DMR-1719875). In addition, characterization was performed at the Cornell NanoScale Facility, an NNCI member supported by NSF grant NNCI-2025233. This work also made use of the Cornell NMR Facility, which was supported, in part, by the NSF through MRI award CHE-1531632. The authors gratefully acknowledge the help from Intel collaborators, Dr. Grant Kloster, Dr. Patrick Theofanis, and Dr. Marie Krysak. In particular, we thank Dr. James Blackwell for very helpful discussions and also helping with various aspects of this work. S.J. and S.B. acknowledge start-up support from Cornell University, including the Robert S. Langer Professorship and the Cornell NEXT Nano Initiative.

REFERENCES

- (1) Felix, N.; Corliss, D.; Petrillo, K.; Saulnier, N.; Xu, Y.; Meli, L.; Tang, H.; De Silva, A.; Hamieh, B.; Burkhardt, M.; Mignot, Y.; Johnson, R.; Robinson, C.; Breton, M.; Seshadri, I.; Dunn, D.; Sieg, S.; Miller, E.; Beique, G.; Labonte, A.; Sun, L.; Han, G.; Verduijn, E.; Han, E.; Kim, B. C.; Kim, J.; Hontake, K.; Huli, L.; Lemley, C.; Hetzer, D.; Kawakami, S.; Matsunaga, K. EUV Patterning Successes and Frontiers; SPIE, 2016; Vol. 9776.
- (2) Goldfarb, D. L. Evolution of patterning materials towards the Moore's Law 2.0 Era. *Jpn. J. Appl. Phys.* **2022**, *61*, SD0802.
- (3) Manouras, T.; Argitis, P. High Sensitivity Resists for EUV Lithography: A Review of Material Design Strategies and Performance Results. *Nanomaterials* **2020**, *10*, 1593.
- (4) Sanders, D. P. Advances in Patterning Materials for 193 nm Immersion Lithography. *Chem. Rev.* **2010**, *110*, 321–360.
- (5) Rothschild, M. Projection optical lithography. *Mater. Today* **2005**, *8*, 18–24.
- (6) Sysova, O.; Durin, P.; Gablin, C.; Léonard, D.; Téolis, A.; Trombotto, S.; Delair, T.; Berling, D.; Servin, I.; Tiron, R.; Bazin, A.; Leclercq, J.-L.; Chevolot, Y.; Soppera, O. Chitosan as a Water-Developable 193 nm Photoresist for Green Photolithography. *ACS Appl. Polym. Mater.* **2022**, *4*, 4508–4519.
- (7) Okoroanyanwu, U.; Shimokawa, T.; Byers, J.; Willson, C. G. Alicyclic Polymers for 193 nm Resist Applications: Synthesis and Characterization. *Chem. Mater.* **1998**, *10*, 3319–3327.
- (8) Pasini, D.; Klopp, J. M.; Fréchet, J. M. J. Design, Synthesis, and Characterization of Carbon-Rich Cyclopolymers for 193 nm Microlithography. *Chem. Mater.* **2001**, *13*, 4136–4146.
- (9) Wagner, C.; Harned, N. Lithography gets extreme. *Nat. Photonics* **2010**, *4*, 24–26.
- (10) Luo, C.; Xu, C.; Lv, L.; Li, H.; Huang, X.; Liu, W. Review of recent advances in inorganic photoresists. *RSC Adv.* **2020**, *10*, 8385–8395
- (11) Ghosh, S.; Pradeep, C. P.; Sharma, S. K.; Reddy, P. G.; Pal, S. P.; Gonsalves, K. E. Recent advances in non-chemically amplified photoresists for next generation IC technology. *RSC Adv.* **2016**, *6*, 74462–74481.
- (12) Li, L.; Liu, X.; Pal, S.; Wang, S.; Ober, C. K.; Giannelis, E. P. Extreme ultraviolet resist materials for sub-7 nm patterning. *Chem. Soc. Rev.* **2017**, *46*, 4855–4866.
- (13) Kruger, S.; Revuru, S.; Higgins, C.; Gibbons, S.; Freedman, D. A.; Yueh, W.; Younkin, T. R.; Brainard, R. L. Fluorinated acid amplifiers for EUV lithography. *J. Am. Chem. Soc.* **2009**, *131*, 9862–9863.
- (14) Kruger, S. A.; Higgins, C.; Cardineau, B.; Younkin, T. R.; Brainard, R. L. Catalytic and Autocatalytic Mechanisms of Acid

- Amplifiers for Use in EUV Photoresists. *Chem. Mater.* **2010**, 22, 5609–5616.
- (15) Arimitsu, K.; Kudo, K.; Ichimura, K. Autocatalytic Fragmentation of Acetoacetate Derivatives as Acid Amplifiers to Proliferate Acid Molecules. *J. Am. Chem. Soc.* **1998**, *120*, 37–45.
- (16) Kim, H.-C.; Park, S.-M.; Hinsberg, W. D. Block Copolymer Based Nanostructures: Materials, Processes, and Applications to Electronics. *Chem. Rev.* **2010**, *110*, 146–177.
- (17) Pfeiffer, F.; Felix, N. M.; Neuber, C.; Ober, C. K.; Schmidt, H.-W. Physical Vapor Deposition of Molecular Glass Photoresists: A New Route to Chemically Amplified Patterning. *Adv. Funct. Mater.* **2007**, *17*, 2336–2342.
- (18) Gibbons, F. P.; Robinson, A. P. G.; Palmer, R. E.; Diegoli, S.; Manickam, M.; Preece, J. A. Fullerene Resist Materials for the 32 nm Node and Beyond. *Adv. Funct. Mater.* **2008**, *18*, 1977–1982.
- (19) De Silva, A.; Felix, N. M.; Ober, C. K. Molecular Glass Resists as High-Resolution Patterning Materials. *Adv. Mater.* **2008**, *20*, 3355–3361
- (20) Ashby, P. D.; Olynick, D. L.; Ogletree, D. F.; Naulleau, P. P. Resist Materials for Extreme Ultraviolet Lithography: Toward Low-Cost Single-Digit-Nanometer Patterning. *Adv. Mater.* **2015**, 27, 5813–5819.
- (21) Tully, D. C.; Trimble, A. R.; Fréchet, J. M. J. Dendrimers with Thermally Labile End Groups: An Alternative Approach to Chemically Amplified Resist Materials Designed for Sub-100 nm Lithography. *Adv. Mater.* **2000**, *12*, 1118–1122.
- (22) Sun, G.; Cho, S.; Clark, C.; Verkhoturov, S. V.; Eller, M. J.; Li, A.; Pavía-Jiménez, A.; Schweikert, E. A.; Thackeray, J. W.; Trefonas, P.; Wooley, K. L. Nanoscopic Cylindrical Dual Concentric and Lengthwise Block Brush Terpolymers as Covalent Preassembled High-Resolution and High-Sensitivity Negative-Tone Photoresist Materials. J. Am. Chem. Soc. 2013, 135, 4203–4206.
- (23) Reichmanis, E.; Houlihan, F. M.; Nalamasu, O.; Neenan, T. X. Chemically amplified resists: Chemistry and processes. *Adv. Mater. Opt. Electron.* **1994**, *4*, 83–93.
- (24) Crivello, J. V.; Shim, S.-Y. Chemically Amplified Electron-Beam Photoresists. *Chem. Mater.* **1996**, *8*, 376–381.
- (25) Crivello, J. V.; Shim, S. Y.; Smith, B. W. Deep-UV Chemically Amplified Dissolution-Inhibited Photoresists. *Chem. Mater.* **1994**, *6*, 2167–2171
- (26) Itani, T.; Kozawa, T. Resist Materials and Processes for Extreme Ultraviolet Lithography. *Jpn. J. Appl. Phys.* **2013**, 52, 010002.
- (27) Kozawa, T.; Tagawa, S. Radiation Chemistry in Chemically Amplified Resists. *Jpn. J. Appl. Phys.* **2010**, *49*, 030001.
- (28) Lee, H.; Park, S.; Kim, M.; Moon, J.; Lee, B.; Cho, M. Multiscale simulation of extreme ultraviolet nanolithography: impact of acid—base reaction on pattern roughness. *J. Mater. Chem. C* **2021**, *9*, 1183—1195.
- (29) Wu, H.; Gonsalves, K. E. Preparation of a Photoacid Generating Monomer and Its Application in Lithography. *Adv. Funct. Mater.* **2001**, *11*, 271–276.
- (30) Wu, H.; Gonsalves, K. E. Novel Positive-Tone Chemically Amplified Resists with Photoacid Generator in the Polymer Chains. *Adv. Mater.* **2001**, *13*, 670–672.
- (31) Stewart, M. D.; Tran, H. V.; Schmid, G. M.; Stachowiak, T. B.; Becker, D. J.; Willson, C. G. Acid catalyst mobility in resist resins. J. Vac. Sci. Technol., B: Nanotechnol. Microelectron.: Mater., Process., Meas., Phenom. 2002, 20, 2946–2952.
- (32) Wang, Q.; Yan, C.; You, F.; Wang, L. A new type of sulfonium salt copolymers generating polymeric photoacid: Preparation, properties and application. *React. Funct. Polym.* **2018**, *130*, 118–125.
- (33) Wang, M.; Yueh, W.; Gonsalves, K. E. New Anionic Photoacid Generator Bound Polymer Resists for EUV Lithography. *Macromolecules* **2007**, *40*, 8220–8224.
- (34) Wang, M.; Jarnagin, N. D.; Lee, C.-T.; Henderson, C. L.; Yueh, W.; Roberts, J. M.; Gonsalves, K. E. Novel polymeric anionic photoacid generators (PAGs) and corresponding polymers for 193 nm lithography. *J. Mater. Chem.* **2006**, *16*, 3701–3707.

- (35) Thackeray, J. W.; Jain, V. J.; Coley, S.; Christianson, M.; Arriola, D.; LaBeaume, P.; Kang, S.-J.; Wagner, M.; Sung, J. W.; Cameron, J. Optimization of Polymer-bound PAG (PBP) for 20nm EUV Lithography. *J. Photopolym. Sci. Technol.* **2011**, *24*, 179–183.
- (36) Hwang, G.-H.; Patil, M.; Seo, S.-K.; Yu, C.-B.; Hur, I.-B.; Kim, D. H.; Shin, C.; Jung, S.-M.; Lee, Y.-H.; Choi, S.-S. Patterning Capability and Limitations by Pattern Collapse in 45 nm and below Node Photo Mask Production; SPIE, 2008; Vol. 7028, p 24.
- (37) Richard, A. L.; David, E. N.; Laren, M. T.; Clifford, L. H. Nonionic photoacid generator behavior under high-energy exposure sources. *J. Micro/Nanolithogr., MEMS, MOEMS* **2009**, *8*, 1–6.
- (38) Kaitz, J. A.; Lee, O. P.; Moore, J. S. Depolymerizable polymers: preparation, applications, and future outlook. *MRS Commun.* **2015**, *5*, 191–204.
- (39) Yardley, R. E.; Kenaree, A. R.; Gillies, E. R. Triggering Depolymerization: Progress and Opportunities for Self-Immolative Polymers. *Macromolecules* **2019**, *52*, 6342–6360.
- (40) Chen, T.; Wang, H.; Chu, Y.; Boyer, C.; Liu, J.; Xu, J. Photo-Induced Depolymerisation: Recent Advances and Future Challenges. *ChemPhotoChem* **2019**, *3*, 1059–1076.
- (41) Lawrie, K.; Blakey, I.; Blinco, J.; Gronheid, R.; Jack, K.; Pollentier, I.; Leeson, M. J.; Younkin, T. R.; Whittaker, A. K. Extreme ultraviolet (EUV) degradation of poly(olefin sulfone)s: Towards applications as EUV photoresists. *Radiat. Phys. Chem.* **2011**, *80*, 236–241.
- (42) Lawrie, K. J.; Blakey, I.; Blinco, J. P.; Cheng, H. H.; Gronheid, R.; Jack, K. S.; Pollentier, I.; Leeson, M. J.; Younkin, T. R.; Whittaker, A. K. Chain scission resists for extreme ultraviolet lithography based on high performance polysulfone-containing polymers. *J. Mater. Chem.* **2011**, 21, 5629–5637.
- (43) Matsuzawa, K.; Mesch, R.; Olah, M.; Wang, W.; Phillips, S.; Willson, C. G. Aromatizing unzipping polyester for EUV photoresist. *Advances in Patterning Materials and Processes XXXII*; SPIE, 2015; Vol. 9425, p 1Q.
- (44) Joo, W.; Wang, W.; Mesch, R.; Matsuzawa, K.; Liu, D.; Willson, C. G. Synthesis of Unzipping Polyester and a Study of its Photochemistry. *J. Am. Chem. Soc.* **2019**, *141*, 14736–14741.
- (45) Engler, A.; Tobin, C.; Lo, C. K.; Kohl, P. A. Influence of material and process parameters in the dry-development of positive-tone, polyaldehyde photoresist. *J. Mater. Res.* **2020**, *35*, 2917–2924.
- (46) Ober, M. S.; Romer, D. R.; Etienne, J.; Thomas, P. J.; Jain, V.; Cameron, J. F.; Thackeray, J. W. Backbone Degradable Poly(aryl acetal) Photoresist Polymers: Synthesis, Acid Sensitivity, and Extreme Ultraviolet Lithography Performance. *Macromolecules* **2019**, *52*, 886–895.
- (47) Rathore, A.; Pollentier, I.; Kumar, S. S.; De Simone, D.; De Gendt, S. Feasibility of unzipping polymer polyphthalaldehyde for extreme ultraviolet lithography. *J. Micro/Nanopatterning, Mater., Metrol.* **2021**, *20*, 034602.
- (48) Deng, J.; Bailey, S.; Jiang, S.; Ober, C. K. High-Performance Chain Scissionable Resists for Extreme Ultraviolet Lithography: Discovery of the Photoacid Generator Structure and Mechanism. *Chem. Mater.* **2022**, *34*, 6170–6181.
- (49) Deng, J.; Bailey, S.; Ober, C. Scissionable polymer photoresist for EUV lithography. *Advances in Patterning Materials and Processes XXXIX*; SPIE, 2022; Vol. 12055, p 132.
- (50) Deng, J.; Kaefer, F.; Bailey, S.; Otsubo, Y.; Meng, Z.; Segalman, R.; Ober, C. K. New Approaches to EUV Photoresists: Studies of Polyacetals and Polypeptoids to Expand the Photopolymer Toolbox. *J. Photopolym. Sci. Technol.* **2021**, *34*, 71–74.
- (51) Deng, J.; Bailey, S.; Ai, R.; Delmonico, A.; Denbeaux, G.; Jiang, S.; Ober, C. K. Synthesis of End-Cap Enabled Self-Immolative Photoresists For Extreme Ultraviolet Lithography. *ACS Macro Lett.* **2022**, *11*, 1049–1054.
- (52) Lutz, J. P.; Davydovich, O.; Hannigan, M. D.; Moore, J. S.; Zimmerman, P. M.; McNeil, A. J. Functionalized and Degradable Polyphthalaldehyde Derivatives. *J. Am. Chem. Soc.* **2019**, *141*, 14544–14548.

- (53) Wang, F.; Diesendruck, C. E. Polyphthalaldehyde: Synthesis, Derivatives, and Applications. *Macromol. Rapid Commun.* **2017**, 39, 1700519.
- (54) Dong, J.; Krasnova, L.; Finn, M. G.; Sharpless, K. B. Sulfur(VI) Fluoride Exchange (SuFEx): Another Good Reaction for Click Chemistry. *Angew. Chem., Int. Ed.* **2014**, *53*, 9430–9448.
- (55) Tsuchimura, T. Recent Progress in Photo-Acid Generators for Advanced Photopolymer Materials. *J. Photopolym. Sci. Technol.* **2020**, 33, 15–26.
- (56) Danilewicz, J. C. Configuration of α -hydroxyimino-ketones. *J. Chem. Soc. C* **1970**, 1049–1052.
- (57) Wu, L.; Bespalov, I.; Witte, K.; Lugier, O.; Haitjema, J.; Vockenhuber, M.; Ekinci, Y.; Watts, B.; Brouwer, A. M.; Castellanos, S. Unravelling the effect of fluorinated ligands in hybrid EUV photoresists by X-ray spectroscopy. *J. Mater. Chem. C* **2020**, 8, 14757–14765.
- (58) Ober, C.; Kafer, F.; Deng, J. Review of essential use of fluorochemicals in lithographic patterning and semiconductor processing. J. Micro/Nanopatterning, Mater., Metrol. 2022, 21, 010901.
- (59) Kaitz, J. A.; Diesendruck, C. E.; Moore, J. S. End group characterization of poly(phthalaldehyde): surprising discovery of a reversible, cationic macrocyclization mechanism. *J. Am. Chem. Soc.* **2013**, 135, 12755–12761.
- (60) Seo, W.; Phillips, S. T. Patterned Plastics That Change Physical Structure in Response to Applied Chemical Signals. *J. Am. Chem. Soc.* **2010**, *132*, 9234–9235.
- (61) Tang, S.; Tang, L.; Lu, X.; Liu, H.; Moore, J. S. Programmable Payload Release from Transient Polymer Microcapsules Triggered by a Specific Ion Coactivation Effect. *J. Am. Chem. Soc.* **2018**, *140*, 94–97.
- (62) Hernandez, H. L.; Kang, S.-K.; Lee, O. P.; Hwang, S.-W.; Kaitz, J. A.; Inci, B.; Park, C. W.; Chung, S.; Sottos, N. R.; Moore, J. S.; Rogers, J. A.; White, S. R. Triggered Transience of Metastable Poly(phthalaldehyde) for Transient Electronics. *Adv. Mater.* **2014**, *26*, 7637–7642.
- (63) Diesendruck, C. E.; Peterson, G. I.; Kulik, H. J.; Kaitz, J. A.; Mar, B. D.; May, P. A.; White, S. R.; Martínez, T. J.; Boydston, A. J.; Moore, J. S. Mechanically triggered heterolytic unzipping of a low-ceiling-temperature polymer. *Nat. Chem.* **2014**, *6*, 623–628.
- (64) Kaitz, J. A.; Moore, J. S. Functional Phthalaldehyde Polymers by Copolymerization with Substituted Benzaldehydes. *Macromolecules* **2013**, *46*, 608–612.
- (65) Bisht, R.; Chattopadhyay, B. Formal Ir-Catalyzed Ligand-Enabled Ortho and Meta Borylation of Aromatic Aldehydes via in Situ-Generated Imines. J. Am. Chem. Soc. 2016, 138, 84–87.
- (66) Carrow, B.; Chen, L. Tri(1-adamantyl)phosphine: Exceptional Catalytic Effects Enabled by the Synergy of Chemical Stability, Donicity, and Polarizability. *Synlett* **2017**, *28*, 280–288.
- (67) Chen, L.; Ren, P.; Carrow, B. P. Tri(1-adamantyl)phosphine: Expanding the Boundary of Electron-Releasing Character Available to Organophosphorus Compounds. J. Am. Chem. Soc. 2016, 138, 6392—6395.
- (68) Tan, Y.; Hartwig, J. F. Palladium-Catalyzed Amination of Aromatic C-H Bonds with Oxime Esters. *J. Am. Chem. Soc.* **2010**, 132, 3676–3677.
- (69) Smedley, C. J.; Homer, J. A.; Gialelis, T. L.; Barrow, A. S.; Koelln, R. A.; Moses, J. E. Accelerated SuFEx Click Chemistry For Modular Synthesis. *Angew. Chem., Int. Ed. Engl.* **2022**, *134*, No. e202112375.
- (70) Kensuke, M.; Ryan, M.; Mike, O.; Wade, W.; Scott, T. P.; Willson, C. G. Aromatizing unzipping polyester for EUV photoresist. *Advances in Patterning Materials and Processes XXXII*; Proc. SPIE, 2015; p 94251Q.
- (71) Fréchet, J. M. J.; Houlihan, F. M.; Bouchard, F.; Kryczka, B.; Wilson, C. G. Design, synthesis, and study of novel, thermally depolymerizable polycarbonates. *J. Chem. Soc., Chem. Commun.* 1985, 1514–1516.
- (72) Yu, A.; Liu, H.; Blinco, J. P.; Jack, K. S.; Leeson, M.; Younkin, T. R.; Whittaker, A. K.; Blakey, I. Patterning of Tailored

- Polycarbonate Based Non-Chemically Amplified Resists Using Extreme Ultraviolet Lithography. *Macromol. Rapid Commun.* **2010**, 31, 1449–1455.
- (73) Mizushima, Y.; Kim, Y.; Nakamura, T.; Uedono, A.; Ohba, T. Behavior of copper contamination on backside damage for ultra-thin silicon three dimensional stacking structure. *Microelectron. Eng.* **2017**, 167, 23–31.
- (74) Satyanarayana, V. S. V.; Kessler, F.; Singh, V.; Scheffer, F. R.; Weibel, D. E.; Ghosh, S.; Gonsalves, K. E. Radiation-Sensitive Novel Polymeric Resist Materials: Iterative Synthesis and Their EUV Fragmentation Studies. ACS Appl. Mater. Interfaces 2014, 6, 4223–4232.
- (75) Gonsalves, K. E.; Wang, M.; Lee, C.-T.; Yueh, W.; Tapia-Tapia, M.; Batina, N.; Henderson, C. L. Novel chemically amplified resists incorporating anionic photoacid generator functional groups for sub-50-nm half-pitch lithography. *J. Mater. Chem.* **2009**, *19*, 2797–2802.
- (76) Wang, M.; Gonsalves, K. E.; Rabinovich, M.; Yueh, W.; Roberts, J. M. Novel anionic photoacid generators (PAGs) and corresponding PAG bound polymers for sub-50 nm EUV lithography. *J. Mater. Chem.* **2007**, *17*, 1699–1706.
- (77) Levinson, H. J. *Principles of Lithography*, 4th ed.; SPIE, 2019; pp 53–102.
- (78) Mack, C. Fundamental Principles of Optical Lithography; John Wiley & Sons, 2007; pp 257–292.
- (79) Spragg, P.; Hurditch, R.; Toukhy, M.; Helbert, J.; Malhotra, S. Reliability of Contrast and Dissolution-Rate-Derived Parameters as Predictors of Photoresist Performance; SPIE, 1991; Vol. 1466, p 283.
- (80) Theodoros, M.; Dimitrios, K.; Eleftherios, K.; Yasin, E.; Maria, V.; Panagiotis, A. *Ultra-sensitive EUV Resists Based on Acid-Catalyzed Polymer Backbone Breaking*; Proc. SPIE, 2018; p 105831R.
- (81) Brainard, R.; Kruger, S.; Higgins, C.; Revuru, S.; Gibbons, S.; Freedman, D.; Yueh, W.; Younkin, T. Kinetics, Chemical Modeling and Lithography of Novel Acid Amplifiers for Use in EUV Photoresists. J. Photopolym. Sci. Technol. 2009, 22, 43–50.
- (82) Cardineau, B.; Garczynski, P.; Earley, W.; Brainard, R. L. Chain-Scission Polyethers for EUV Lithography. *J. Photopolym. Sci. Technol.* **2013**, *26*, 665–671.
- (83) Kubota, N.; Hayashi, T.; Iwai, T.; Komano, H.; Kawai, A. Advanced Resist Design Using AFM Analysis for ArF Lithography. *J. Photopolym. Sci. Technol.* **2003**, *16*, 467–474.
- (84) Yoshimura, T.; Shiraishi, H.; Yamamoto, J.; Okazaki, S. Nano edge roughness in polymer resist patterns. *Appl. Phys. Lett.* **1993**, *63*, 764–766.
- (85) Yoshimura, T.; Shiraishi, H.; Yamamoto, J.; Okazaki, S. Correlation of Nano Edge Roughness in Resist Patterns with Base Polymers. *Jpn. J. Appl. Phys.* **1993**, 32, 6065–6070.
- (86) Liu, E.; Hegazy, A.; Choi, H.; Weires, M.; Brainard, R.; Denbeaux, G. Characterization of Surface Variation of Chemically Amplified Photoresist to Evaluate Extreme Ultraviolet Lithography Stochastics Effects. *J. Photopolym. Sci. Technol.* **2021**, *34*, 63–70.
- (87) Richard, A. L.; David, E. N.; Laren, M. T.; Clifford, L. H. Nonionic PAG behavior under high energy exposure sources. *Advances in Resist Materials and Processing Technology XXVI*; SPIE, 2009; Vol. 7273, p 1R.
- (88) Cheng-Tsung, L.; Mingxing, W.; Kenneth, E. G.; Wang, Y.; Jeanette, M. R.; Todd, R. Y.; Clifford, L. H. Effect of PAG and matrix structure on PAG acid generation behavior under UV and high-energy radiation exposure. Advances in Resist Materials and Processing Technology XXV; SPIE, 2008; Vol. 6923, p 2F.
- (89) Yamashita, K.; Kamimura, S.; Takahashi, H.; Nishikawa, N. A Resist Material Study for LWR and Resolution Improvement in EUV Lithography. *J. Photopolym. Sci. Technol.* **2008**, *21*, 439–442.
- (90) Jonathan, H. M.; Han, W.; David, G. P.; Andrew, R. N.; Patrick, P. N. Investigating extreme ultraviolet radiation chemistry with first-principles quantum chemistry calculations. *J. Micro/Nanolithogr., MEMS, MOEMS* **2020**, *19*, 1–11.
- (91) Grimme, S.; Hansen, A. A Practicable Real-Space Measure and Visualization of Static Electron-Correlation Effects. *Angew. Chem., Int. Ed.* **2015**, *54*, 12308–12313.

- (92) Kanai, Y.; Wang, X.; Selloni, A.; Car, R. Testing the TPSS metageneralized-gradient-approximation exchange-correlation functional in calculations of transition states and reaction barriers. *J. Chem. Phys.* **2006**, *125*, 234104.
- (93) Caldeweyher, E.; Mewes, J. M.; Ehlert, S.; Grimme, S. Extension and evaluation of the D4 London-dispersion model for periodic systems. *Phys. Chem. Chem. Phys.* **2020**, 22, 8499–8512.
- (94) Mardirossian, N.; Head-Gordon, M. Mapping the genome of meta-generalized gradient approximation density functionals: The search for B97M-V. *J. Chem. Phys.* **2015**, *142*, 074111.